are bounded to the southeast by hummocky rolling plains. Although the southwest portion of feature A is somewhat indistinct, it appears to extend slightly into the mysterious cantaloupe terrain, being bounded there by a prominent linear ridge. Within the boundaries of the quasi-circular features are many smaller structures of almost certain cryovolcanic origin (*1, 5, 6*). These include two of only three examples of "lake-like" features visible in Voyager images of Triton. The smooth floors and terraced edges of the lake-like features are thought to have been emplaced by multiple episodes of icy volcanic flooding. The entire region is dominated by high-standing smooth materials that appear to have erupted from smaller quasi-circular depressions and extruded in flows several kilometers thick with rounded margins (*1*). Other proposed cryovolcanic formations in the region are irregular pits and pit chains, interpreted as explosive cryovolcanic vents, and dark lobate flowlike features (*5*).

There are at least two possible interpretations of the quasi-circular features. Smith *et al.* (*7*) used the term "palimpsest" to describe a class of roughly circular, large (>50 km) albedo markings on Ganymede and Callisto that are interpreted to be vestigial remains of impact craters that have undergone nearly complete viscous relaxation or that formed as a result of impacts into a fluid mantle (*8*). Palimpsests are generally higher in albedo than their surrounding terrains and exhibit little topographic relief at scales larger than a few kilometers. The quasi-circular features are reminiscent of palimpsests because of their large sizes, crudely circular planform, and subdued broad-scale topography. Unlike palimpsests on the Jovian satellites, these features are generally lower in albedo than their surrounding terrain and lack the characteristic small-scale topographic structure of palimpsests such as hummocky ejecta mantles, basin-related massifs or scarps, or rimmed furrows like Callisto's Valhalla structure (*7, 9*). In addition, the quasi-circular features lie within terrains that are interpreted to be geologically youthful (*1, 5, 10*) because of their paucity of identifiable impact craters. On other planets and satellites, impact structures that are similar in scale to the quasi-circular features are interpreted to be ancient, dating back to the time of terminal bombardment, some 3.5 billion to 4.0 billion years ago. Thus, the interpretation of Triton's large quasi-circular features as possible palimpsests is difficult to reconcile with accepted interpretations of the satellite's geological history.

A more tenable explanation, proposed by Croft (*11*), is that the features are a result of regional cryovolcanic activity. This hypothesis is supported by detailed geological mapping and analyses of high-resolution images of Triton (*1, 5, 6*) that have ascribed cryovolcanic origins to numerous smaller scale structures in this region of the satellite's surface. The overall pattern of the quasi-circular features may be due to an ancient buried impact basin or to an upwelling convective mantle plume. There is presently no clear evidence that the regional topography of quasi-circular features is either elevated or depressed relative to surrounding terrains. The complexity of superposed landforms suggests that the quasi-circular features were emplaced not in a single, massive event but instead by many smaller events concentrated over a regional "hot spot." Thus far, comparable features have not been identified on any other icy satellite.

REFERENCES AND NOTES

1. B. A. Smith *et al.*, *Science* **246**, 1422 (1989).
2. J. Hillier *et al.*, *J. Geophys. Res.* **96**, 19203 (1991).
3. P. Lee *et al.*, in preparation.
4. L. A. Soderblom *et al.*, *Science* **250**, 410 (1990).
5. S. K. Croft, *Lunar Planet Sci. Conf.* **XXI**, 244 (1990); *ibid.*, p. 246; *ibid.*, p. 248.
6. J. Kargel and R. Strom, *ibid.*, p. 599.
7. B. A. Smith *et al.*, *Science* **206**, 927 (1979).
8. P. Thomas and S. Squyres, *J. Geophys. Res.* **95**, 19161 (1990).
9. Q. R. Passey and E. M. Shoemaker, in *Satellites of Jupiter*, D. Morrison, Ed. (Univ. of Arizona Press, Tucson, 1982), pp. 379–434.
10. R. G. Strom, S. K. Croft, J. M. Boyce, *Science* **250**, 437 (1990).
11. S. K. Croft, personal communication.

12. We are indebted to two anonymous referees and especially S. K. Croft for constructive reviews. We thank B. Boettcher and J. Hovencamp for help with illustrations and M. Roth for manuscript preparation. This study was funded by National Aeronautics and Space Administration grants NAGW-2084 and NAGW-2186.

10 June 1991; accepted 19 November 1991

Channel Initiation and the Problem of Landscape Scale

DAVID R. MONTGOMERY* AND WILLIAM E. DIETRICH

Since the 1940s it has been proposed that landscape dissection into distinct valleys is limited by a threshold of channelization that sets a finite scale to the landscape. This threshold is equal to the hillslope length that is just shorter than that necessary to support a channel head. A field study supports this hypothesis by showing that an empirically defined topographic threshold associated with channel head locations also defines the border between essentially smooth, undissected hillslopes and the valley bottoms to which they drain. This finding contradicts assertions that landscapes are scale-independent and suggests that landscape response to changes in climate or land use depends on the corresponding changes in the threshold of channelization.

MOST GEOLOGIC AGENTS OF EROSION modify the land surface on a variety of spatial scales. Consequently, casual observation of topographic maps, or observations of landscapes from afar, suggest that landscapes are scale-independent (Fig. 1). Indeed, fractal analyses of landscape form have revived the hypothesis that there is no characteristic scale to the landscape and that finer and finer scales of dissection will be found upon closer and closer inspection (*1*). In contrast, detailed topographic maps reveal that there is an internal structure to the landscape expressed as ridges and valleys of finite size and that the scale of this limit to landscape dissection varies in different landscapes (Fig. 1). Gilbert (*2*) first recognized the apparent finite extent to landscape dissection, and Horton (*3*) proposed that this dissection proceeds until hillslope lengths are everywhere just shorter than that which could generate sufficient overland flow to initiate surface erosion and, consequently, channelization. Subsequently, several workers have proposed models to explain channelization and landscape development on the basis of thresholds of erosion (*3–6*). An alternative theory for finite dissection, first proposed by Smith and Bretherton (*7*), states that hillslopes are unstable to lateral perturbations in which advective (*8*) dominates diffusive sediment transport (*9*). A channelization threshold, however, has not been shown to distinguish hillslopes from valleys in a real rather than a model landscape. We present field data that demonstrate that drainage basins tend to be geometrically similar (contributing to a scale-independent landscape appearance) but that finite dissection of the landscape corresponds to the lower bound of an empirically determined topographic threshold for channelization.

Department of Geology and Geophysics, University of California, Berkeley, CA 94720.

*Present address: Department of Geological Sciences, University of Washington, Seattle, WA 98195.

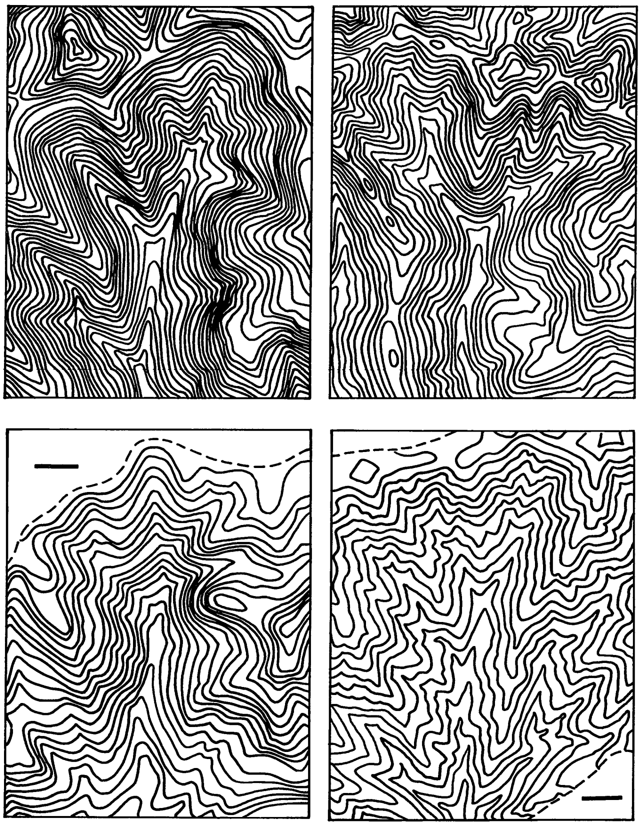

Fig. 1. Without a scale bar it is almost impossible to determine even the approximate scale of a topographic map. The upper two maps show adjacent drainage basins in the Oregon Coast Range and illustrate the effect of depicting an area of similar topography at different scales. The map on the right covers an area four times as large as, and has twice the contour interval of, the map on the left. The lower two maps depict very different landscapes, and detailed mapping was done to resolve the finest scale valleys, which determine the extent, or scale, of landscape dissection. The map on the left shows a portion of a small badlands area at Perth Amboy, New Jersey (*28*) (scale bar represents 2 m; contour interval is 0.3 m). The map on the right shows a portion of the San Gabriel Mountains of southern California (*20*) (scale bar represents 100 m; contour interval is 15 m). Dashed lines on both lower maps represent the limit of original mapping. The drainage basin outlet on each map is oriented toward the bottom of the page. All four maps suggest a limit to landscape dissection, defined by the size of the hillslopes separating valleys. This apparent limit, however, only corresponds to the extent of valley dissection definable in the field for the case of the lower two maps.

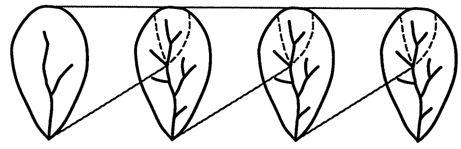

Fig. 3. The coherence of the data in Fig. 2 across 11 orders of magnitude indicates a geometric similarity between small drainage basins and the larger drainage basins that contain them. Although the variance about the trend in Fig. 2 indicates a range in individual basin shapes, this general relation apparently characterizes the landscape down to the finest scale of convergent topography.

We collected data from small drainage basins in a variety of geologic settings that represent a range in climate and vegetation (*4, 5*). We measured the drainage area (A), basin length (L), and local slope (S) for locations in convergent topography along low-order channel networks, at channel heads, and along unchanneled valleys in drainage basins where we had mapped the channel networks in the field (*4, 5*). Drainage area was defined as the area upslope of the measurement location, basin length was defined as the length along the main valley axis to the drainage divide, and local slope was measured in the field. The structural relation of drainage area to basin length (*10*) for our composite data set is

$$L = 1.78\,A^{0.49} \tag{1}$$

where L and A are expressed in meters. This relation is well approximated by the simple, isometric relation

$$L \approx (3\,A)^{0.5} \tag{2}$$

Inclusion of reported drainage area and mainstream length data from larger networks (*11–15*) provides a composite data set that also is reasonably fit (*5*) by this relation. The data span a range of more than 11 orders of magnitude in basin area, from unchanneled hillside depressions to the world's largest rivers (Fig. 2). This relation suggests that there is a basic geometric similarity between drainage basins and the smaller basins contained within them that holds down to the finest scale to which the landscape is dissected (Fig. 3). In the field this scale is easily recognized as that of the topographically divergent ridges that separate these fine-scale valleys.

Equation 1 differs, however, from the relation between the mainstream length and drainage area first reported by Hack (*11*), in which basin area increases as $L^{0.6}$. Many subsequent workers interpreted similar relations as indicating that drainage network planform geometry changes with increasing scale. Relations between mainstream length and drainage area also have been used to infer the fractal dimension of individual channels and channel networks (*1, 16*). Mueller (*15*), however, reported that the exponent in the relation of mainstream length to drainage area is not constant, but decreases from 0.6 to ~0.5 with increasing network size, and Hack (*11*) noted that the exponent in this relation varies for individual drainage networks. We cannot compare our data more quantitatively with those reported by others because the mainstream length will diverge from the basin length in proportion to the area upslope of the stream head. We suspect that the difference in the relations derived from our data and those reported previously reflects variation in the headward extent of the stream network depicted on maps of varying scale (*17*) as well as downstream variations in both channel sinuosity (*14*) and drainage density (*18*). The general scale independence indicated in Fig. 2 suggests that landscape dissection results in an integrated network of valleys that capture geometrically similar drainage basins at scales ranging from the largest rivers to the finest scale valleys. Within this scale range there appears to be little inherent to the channel network and to the corresponding shape of the drainage area it captures that provides reference to an absolute scale.

Nonetheless, field studies in semiarid to humid regions demonstrate that there is a finite extent to the branching channel network (*4, 5, 19–22*). Channels do not occupy the entire landscape; rather, they typically begin at the foot of an unchanneled valley,

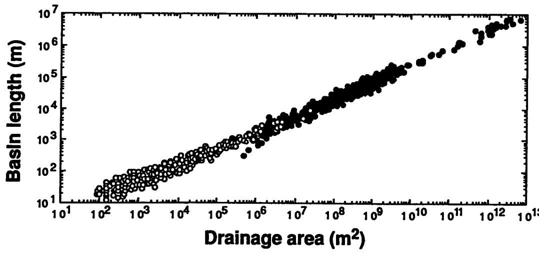

Fig. 2. Basin length versus drainage area for unchanneled valleys, source areas, and low-order channels mapped in this study (○) and mainstream length versus drainage area data reported for large channel networks (●). Sources of mainstream length data are given in (*5*).

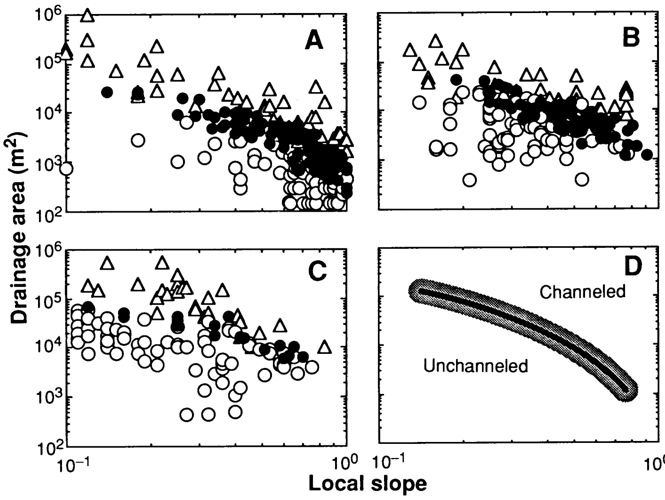

Fig. 4. Drainage area versus local slope for channel heads (●), unchanneled valleys (○), and low-order channel networks (△) from study areas in (**A**) coastal Oregon, (**B**) northern California, and (**C**) southern California (*29*). Local slope was measured in the field, and drainage area was determined from topographic base maps. (**D**) In these field areas, data from channel heads define a threshold between channeled and unchanneled regions of the landscape. Threshold-based channel initiation models predict that the form of this transition will reflect different channel initiation processes (*5*). The central tendency (black line) will reflect the general environmental controls on channel initiation (for example, climate and vegetation). The variance about this relation (shading) is controlled by spatial and short-term temporal variability in the factors influencing these processes (*4, 5*).

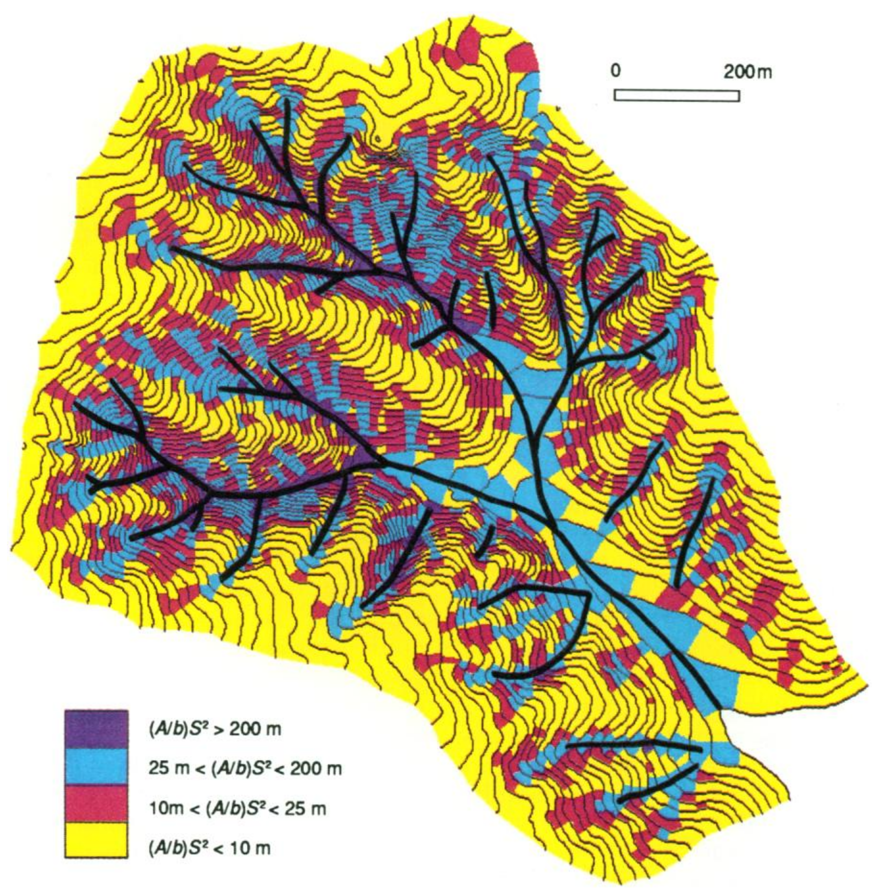

Fig. 5. Distribution of values of $(A/b)S^2$ for a portion of the northern California study area (contour interval is 5 m). Black lines represent the channel network mapped in the field (*4*). Areas that plot above the upper limit of the source area–slope envelope in Fig. 4B [$(A/b)S^2 > 200$ m)] are channeled valleys; areas within the range in values defined by the source area–slope envelope [25 m < $(A/b)S^2$ < 200 m)] are transitional areas in which channel heads occur; areas that plot just below the lower limit of the source area–slope relation [10 m < $(A/b)S^2$ < 25 m)], and thus just below the threshold of channelization, are the base of hillslopes and the upslope ends of valleys; and areas significantly below the lower bound to the source area–slope envelope [$(A/b)S^2$ < 10 m)] are smooth, undissected ridgetops. The transitional areas correspond to areas mapped in the field as containing Holocene colluvial or alluvial fills, areas with thin soils, and bedrock outcrops exposed at the base of steep hillslopes. Threshold areas border and essentially surround transitional areas, indicating that the channel network extends throughout the landscape to a limit imposed by the drainage area–slope threshold for channel initiation. Further applications of this approach are presented elsewhere (*26*).

and the location of the channel head shifts in response to climatic and land-use changes (*4, 5, 22*). In landscapes where deep-seated landsliding and dissolution processes are minor geomorphic agents, valleys are formed by concentrated runoff and erosion in channels and (in steeper valleys) by the periodic scour of debris flows. The intervening hillslopes are shaped by diffusive sediment transport processes (for example, soil creep, rain splash, and biological activity). Field data indicate that the scale of landscape dissection and the limit to the scale-independent geometry suggested in Fig. 2 reflect the transition from sediment transport by hillslope to channel processes.

Our data from three study areas in the Coast Ranges of the western United States (Fig. 4) show that an inverse relation between the drainage area contributing to a channel head (source area) and the local valley slope (*4, 5*) defines a topographic threshold between channeled and unchanneled regions of the landscape (*23*). The observed inverse relations exhibit forms expected from threshold-based channel initiation theories for landsliding (*4, 21*) (Fig. 4A) and overland flow (*5*) (Fig. 4, B and C). These data demonstrate that channel heads lie at a transition between channeled and unchanneled portions of the landscape but that for any given slope the source-area size may vary by as much as an order of magnitude. This scatter probably arises from both spatial and temporal variation in the hydrologic and erosional processes governing channel initiation and should introduce considerable variation into channel and valley development, thus contributing a random aspect to the appearance of many landscapes.

An empirical test for a relation among topographic thresholds, channel initiation, and the degree of landscape dissection would be to see if this threshold also leads to a lower bound to valley development. The relation between channel initiation and landscape dissection is difficult to study empirically because climatic and land-use shifts have affected the current location of the channel head in most places, and it is difficult to demonstrate equilibrium. In some areas, however, it is possible to argue for a linkage between contemporary channel head locations and landscape dissection. For example, the channel network in the Tennessee Valley area in Marin County, California (the area represented in Fig. 4B), was aggrading throughout the Holocene (*5*), which was drier than the glacial climate in this region (*24*). Recent channel advance due to cattle grazing in the last 150 years (*5*) has compensated somewhat for the climatically driven Holocene retraction of the channel network. Nearly all channel heads are downslope of a single unchanneled valley rather than downslope of an extensive network of unchanneled valleys. Consequently, we speculate that the channel head locations in this area approximate a condition of contributing slope and drainage area of long-term geomorphic significance.

To test the threshold hypothesis for landscape dissection at this study site, we determined a relation for the upper and lower range of channel heads in Fig. 4B, used a digital terrain model (*25*) to define the upslope drainage area and ground slope for roughly 20-m^2 elements of a 1.2-km^2 basin, and then plotted the spatial distribution of elements lying well below, close to, within, and above the data range for channel heads. Upper and lower bounds to the range in channel head locations are defined by the relations

$$AS^2 = 4000 \text{ m}^2 \quad (3)$$

$$AS^2 = 500 \text{ m}^2 \quad (4)$$

The digital terrain model was used to divide the modeled land surface into discrete elements by drawing the equivalent of flow lines across the contours from valley bottoms to drainage divides at a specified interval. Because measured elevation points are distributed at an ~10-m spacing (*26*), we selected 20 m as a reasonably small interval for the flow lines. This resulted in 5632 individual elements, defined by a pair of contour lines on the upslope and downslope sides of the element and a stream line on each lateral boundary. In order to minimize the effect of element size on the analysis, we divided the areas in Eqs. 3 and 4 by 20 m and used the resulting relations to analyze topographic threshold patterns relative to the extent of the valley network:

$$(A/b)S^2 = 200 \text{ m} \quad (5)$$

$$(A/b)S^2 = 25 \text{ m} \quad (6)$$

where A/b is the drainage area per unit contour length.

The analysis showed that the entire channel network and nearly all of the unchanneled valleys (areas of concave contours above and tributary to the channeled valleys) lie either within or above the channel head threshold range (Fig. 5). The hillslopes bordering the channels, and lying at the heads of unchanneled valleys, are consistently just below the topographic threshold (*27*). Field inspection indicates that although some fine-scale valleys are not represented in the topographic map of Fig. 5, these valleys lie either within, or very close to, areas predicted to be within the variance for channel head locations. The ridge lines are well below this threshold everywhere. We interpret the relations shown in Fig. 5 as strong evidence that the topographic conditions setting the threshold to channelization also define the limit of valley dissection and, consequently, the hillslope length.

Although our results support the threshold hypothesis of landscape development, they do not refute the alternative model for dissection limitation originally set forth by Smith and Bretherton (*7*). They proposed that landscape dissection proceeds until the hillslopes are dominated everywhere by diffusive sediment-transport processes, which result in convex slope profiles that are stable to random topographic perturbations that would grow into valleys. Their model predicts that concave topography will be unstable to even infinitesimal perturbations, and only recently (*8*) has progress been made in understanding quantitatively what sets finite amplitude perturbations. Although the Smith and Bretherton hypothesis suggests that the transition from unchanneled to channeled portions of the landscape should correspond to the convex to concave transition downslope along a hillslope profile, further development of this theory is needed to guide field tests of this hypothesis. A similar transition, however, would likely form from variation in channel head locations along valleys in response to changes in the factors controlling the threshold of channelization.

A threshold-based limit to landscape dissection links the development of channel networks, valleys, and hillslopes and implies that there is a hysteresis in the response of a landscape to changes in the factors influencing channel initiation. This hysteresis, in part, makes testing of this hypothesis difficult. If climate change or land disturbance decreases the drainage area necessary to initiate a channel, then expansion of the channel network into unchanneled valleys and incision into hillsides will result. In contrast, an increase in the drainage area necessary to sustain a channel will result in local infilling of valley heads and the development of dry valleys, or hollows, only at the upslope ends of the channel network. Furthermore, channels or rills may be carved into unchanneled valleys and hillslopes relatively quickly when the threshold for channel initiation is decreased, but significant time may be required to infill valleys when the threshold for channel initiation increases. Such a time lag between process and form reflects the relative magnitude of processes acting to round and incise the landscape. Because these processes may change faster than the landscape can respond, an equilibrium condition will most likely never be strictly achieved in natural landscapes. Consequently, our results point to the need to focus on processes controlling the location of the channel head for both practical problems, such as predicting landscape response to urbanization, agricultural practices, and climate change, and the theoretical problems of predicting landscape morphology and evolution.

REFERENCES AND NOTES

1. W. M. Davis, *Geogr. J.* **14**, 481 (1899); B. B. Mandelbrot, *The Fractal Geometry of Nature* (Freeman, New York, 1983); D. G. Tarboton, R. L. Bras, I. Rodriguez-Iturbe, *Water Resour. Res.* **24**, 1317 (1988).
2. G. K. Gilbert, *Geology of the Henry Mountains* (U.S. Geographic and Geologic Survey, Washington, DC, 1877); *J. Geol.* **17**, 344 (1909).
3. R. E. Horton, *Geol. Soc. Am. Bull.* **56**, 275 (1945).
4. D. R. Montgomery and W. E. Dietrich, *Nature* **336**, 232 (1988); *Water Resour. Res.* **25**, 1907 (1989).
5. D. R. Montgomery, thesis, University of California, Berkeley (1991).
6. G. R. Willgoose, thesis, Massachusetts Institute of Technology (1989); ———, R. L. Bras, I. Rodriguez-Iturbe, *Earth Surf. Process. Landf.* **16**, 237 (1991); *Water Resour. Res.* **27**, 1671 (1991).
7. T. R. Smith and F. P. Bretherton, *Water Resour. Res.* **8**, 1506 (1972).
8. D. S. Loewenherz, *J. Geophys. Res.* **96**, 8453 (1991).
9. M. J. Kirkby [in *Thresholds in Geomorphology*, D. R. Coates and J. D. Vitek, Eds. (Allen & Unwin, Boston, 1980), pp. 53–73; in *Geomorphological Models*, F. Ahnert, Ed. (Catena, Cremlingen-Destedt, Federal Republic of Germany, 1987), pp. 1–14] also has argued that this transition in sediment-transport dominance determines the extent of landscape dissection.
10. We use the structural relation rather than regression because measurements of both basin area and basin length are subject to error [D. M. Mark and M. Church, *Math. Geol.* **9**, 63 (1977)].
11. J. T. Hack, *U.S. Geol. Surv. Prof. Pap. 294B* (1957).
12. W. B. Langbein, *U.S. Geol. Surv. Water Supply Pap. 968C* (1947); A. B. Taylor and H. E. Schwarz, *Eos* **33**, 235 (1952); L. M. Brush, *U.S. Geol. Surv. Prof. Pap. 282F* (1961); D. M. Gray, *J. Geophys. Res.* **66**, 1215 (1961); L. B. Leopold, M. G. Wolman, J. P. Miller, *Fluvial Processes in Geomorphology* (Freeman, San Francisco, 1964); J. E. Mueller, *Geol. Soc. Am. Bull.* **83**, 3471 (1972); P. C. Patton and V. R. Baker, *Water Resour. Res.* **12**, 941 (1976); P. E. Potter, *J. Geol.* **86**, 13 (1978); R. C. Kochel, A. D. Howard, C. McLane, in *Models in Geomorphology*, M. J. Woldenberg, Ed. (Allen & Unwin, Winchester, MA, 1985), pp. 313–341.
13. L. B. Leopold and J. P. Miller, *U.S. Geol. Surv. Prof. Pap. 282A* (1956).
14. J. S. Smart and A. J. Surkan, *Water Resour. Res.* **3**, 963 (1967).
15. J. E. Mueller, *Geol. Soc. Am. Bull.* **84**, 3127 (1973).
16. A. T. Hjelmfelt, *Water Resour. Bull.* **24**, 455 (1988); R. Rosso, B. Bacchi, P. LaBarbera, *Water Resour. Res.* **27**, 381 (1991).
17. A. Robert and A. G. Roy, *Water Resour. Res.* **26**, 839 (1990).
18. R. L. Shreve, *ibid.* **10**, 1167 (1974).
19. M. A. Melton, *Tech. Rep. 11 Off. Nav. Res. Proj. 389-042* (1957); M. Morisawa, *Eos* **38**, 86 (1957); J. T. Hack and J. C. Goodlett, *U.S. Geol. Surv. Prof. Pap.* 347 (1960); W. E. Dietrich and T. Dunne, *Z. Geomorphol. Suppl.* **29**, 191 (1978).
20. J. C. Maxwell, *Tech. Rep. 19 Off. Nav. Res. Proj. 389-042* (1960).
21. W. E. Dietrich, C. J. Wilson, S. L. Reneau, in *Hillslope Processes*, A. D. Abrahams, Ed. (Allen & Unwin, Boston, 1986), pp. 361–388.
22. S. L. Reneau, W. E. Dietrich, R. I. Dorn, C. R. Berger, M. Rubin, *Geology* **14**, 655 (1986); W. E. Dietrich, S. L. Reneau, C. J. Wilson, *Int. Assoc. Hydrol. Sci. Publ.* **165**, 27 (1987).
23. Figure 4 differs substantially from our earlier findings (*4*), because with the inclusion of data from

channels and unchanneled valleys, as well as from channel heads, these plots demonstrate that channel head locations define a threshold transition between channeled and unchanneled regions of the landscape. See (*4*) for further discussion of field techniques and criteria used to define channel head locations.
24. D. L. Johnson, *Quat. Res.* (*N.Y.*) **8**, 154 (1977); J. D. Sims, Ed., *Geol. Soc. Am. Spec. Pap. 214* (1988); COHMAP members (P. M. Anderson *et al.*), *Science* **241**, 1043 (1988); S. Rypins, S. L. Reneau, R. Byrne, D. R. Montgomery, *Quat. Res.* (*N.Y.*) **32**, 72 (1989).
25. We used the model TOPOG [E. M. O'Loughlin, *Water Resour. Res.* **22**, 794 (1986)] to create a digital land surface from topography digitized from low-altitude stereo air photographs.
26. W. E. Dietrich, C. J. Wilson, D. R. Montgomery, J. McKean, R. Bauer, in preparation.
27. The lower limit to the range selected to illustrate areas just below the threshold zone in Fig. 5 is arbitrary. The range depicted was selected to illustrate that areas marginally below the channelization threshold range essentially surround areas of convergent topography. These zones expand upslope if a wider range in values is used and contract toward the margins of the channel network if a more restrictive range is adopted. Some of the areas depicted as in the transition zone are steep areas underlain by thin soil profiles or areas of bedrock outcrop in which the processes influencing channel initiation differ from the rest of the soil-mantled drainage basin. In general, however, the transition zones should define those parts of the landscape most sensitive to environmental change, an interpretation supported by a close correspondence with the extent of Holocene valley fills.
28. S. A. Schumm, *Geol. Soc. Am. Bull.* **67**, 597 (1956).
29. The coastal Oregon study area consists of 12 second- and third-order basins near Coos Bay, Oregon. The area is covered by a managed forest and underlain by relatively undeformed Tertiary sandstone. The northern California study area is composed of four adjacent second- to fourth-order basins in the Tennessee Valley area north of San Francisco, California. The area is covered by coastal scrub and grassland vegetation and is underlain by highly deformed Mesozoic sandstone, chert, and greenstone of the Franciscan Assemblage. The southern California study area consists of two third-order basins located in the southern Sierra Nevada about 45 km east of Bakersfield, California. The area is covered with an open oak forest and is underlain by Mesozoic granitic rocks. Further descriptions of the study areas, and the channel initiation processes acting within them, are in (*4, 5*).
30. This research was funded by NSF grants EAR-8451175 and EAR-8917467. We thank J. McKean for digitizing the elevation data for Tennessee Valley; C. J. Wilson and R. Reiss for assistance with TOPOG; and W. Rankin, the Golden Gate National Recreation Area, and the Weyerhaeuser Company for access to our study areas. We also thank J. Kirchner, C. J. Wilson, D. Tarboton, and several reviewers for commenting on drafts of this manuscript.

7 August 1991; accepted 25 November 1991

Electrical Transport Properties of Undoped CVD Diamond Films

L. S. PAN,* D. R. KANIA, S. HAN, J. W. AGER III, M. LANDSTRASS, O. L. LANDEN, P. PIANETTA

Polycrystalline diamond films synthesized by microwave-assisted chemical vapor deposition (MACVD) were examined with transient photoconductivity, and two fundamental electrical transport properties, the carrier mobility and lifetime, were measured. The highest mobility measured is 50 centimeters squared per volt per second at low initial carrier densities (<10^{15} per cubic centimeter). Electron-hole scattering causes the carrier mobility to decrease at higher carrier densities. Although not measured directly, the carrier lifetime was inferred to be 40 picoseconds. The average drift length of the carriers is smaller than the average grain size and appears to be limited by defects within the grains. The carrier mobility in the MACVD films is higher than values measured in lower quality dc-plasma films but is much smaller than that of single-crystal natural diamond.

With the development of synthetic diamond films made by chemical vapor deposition (CVD), diamond devices have been envisioned for consumer and industrial products such as space applications, process control equipment, electric power installations, and automobiles. Diamond electronic devices would be ideally suited for applications associated with high power, high frequency, high temperatures, and harsh radiation environments. This is clear from the extreme physical and electronic properties of diamond. Single-crystal natural diamond has the highest room-temperature thermal conductivity (20 W cm^{-1} K^{-1}) (*1*), the lowest coefficient of thermal expansion (0.8×10^{-6}) (*2*), the highest electron- and hole-saturated velocities (1.5×10^7 cm s^{-1} and 1.05×10^7 cm s^{-1}, respectively) (*3*), the highest electrical breakdown field (10^7 V cm^{-1}) (*4*), a low dielectric constant (5.7) (*5*), high intrinsic resistivity (as high as 10^{20} ohm-cm) (*6*), and high electron and hole mobilities (~2000 and 1200 cm^2 V^{-1} s^{-1}, respectively). In addition, diamond is chemically inert and radiation-hard. The Keyes (*7*) and Johnson (*8*) figures of merit for diamond are nearly two orders of magnitude better than that for silicon. Simple prototype diamond devices, such as *p-n* junction diodes and transistors containing both natural and synthetic diamond, have been fabricated [see (*9*)].

The recent growing interest in diamond stems from significant advances in the growth of synthetic diamond films made by CVD, which have led to films of large area and thickness and of improved quality (*10*). In the CVD method, a gas mixture containing C and H is excited to form a plasma. A typical gas mixture contains ~1% methane and ~99% H_2. Under certain gas pressure and substrate temperature ranges (typically 20 to 100 torr and 700° to 950°C, respectively), graphitic (sp^2-bonded) C growth is suppressed, while diamond-bonded (sp^3-bonded) C is successfully deposited. Films with little or no nondiamond-bonded C can now be deposited on a variety of substrates.

All CVD films deposited on nondiamond substrates to date are polycrystalline. Even so, the electrical and optical properties of CVD films are approaching those of natural diamond. For example, the resistivity of natural insulating diamond is typically greater than 10^{15} ohm-cm, and values as high as 10^{13} ohm-cm have been achieved in CVD films (*11*). Being able to produce CVD films with high resistivity is promising, but resistivity alone does not determine whether a material is suitable for electronic applications because the resistivity can depend on carrier concentration, carrier mobility, and space charge (*12*). Traditional characterization uses the Hall effect to determine both the mobility and the concentration of the carriers, but in undoped, insulating materials this measurement is difficult because of the low intrinsic carrier concentration (*13*).

A powerful technique that is suitable for characterizing such resistive materials is transient photoconductivity (PC), in which a known carrier concentration is created by intrinsic photoexcitation. From the magnitude of the photocurrent and its transient decay, two fundamental properties for device applications, the mobility and lifetime of the carriers, can be determined. This technique has been applied to natural IIa diamonds (*14*). In this report we discuss results on CVD polycrystalline diamond

L. S. Pan and P. Pianetta, Stanford Synchrotron Radiation Laboratory, Stanford Linear Accelerator Center Bin 99, Post Office Box 4349, Stanford, CA 94309.
D. R. Kania, S. Han, O. L. Landen, Lawrence Livermore National Laboratory, L-473, Post Office Box 5508, Livermore, CA 94550.
J. W. Ager III, Center for Advanced Materials, Lawrence Berkeley Laboratory, University of California, Berkeley, CA 94720.
M. Landstrass, Crystallume, 125 Constitution Avenue, Menlo Park, CA 94025.

*To whom correspondence should be addressed at Lawrence Livermore National Laboratory, L-476, Post Office Box 5508, Livermore, CA 94550.